Molecular Simulation of Thermo-osmotic Slip

Raman Ganti,[1,*] Yawei Liu,[2] and Daan Frenkel[1,†]

[1]*Department of Chemistry, University of Cambridge, Lensfield Road, Cambridge CB2 1EW, United Kingdom*
[2]*Beijing University of Chemical Technology, Beijing 100029, People's Republic of China*

Thermo-osmotic slip—the flow induced by a thermal gradient along a surface—is a well-known phenomenon, but curiously there is a lack of robust molecular-simulation techniques to predict its magnitude. Here, we compare three different molecular-simulation techniques to compute the thermo-osmotic slip at a simple solid-fluid interface. Although we do not expect the different approaches to be in perfect agreement, we find that the differences are barely significant for a range of different physical conditions, suggesting that practical molecular simulations of thermo-osmotic slip are feasible.

Thermo-osmosis and thermophoresis are phenomena of great practical interest in the context of nonisothermal hydrodynamics [1,2], nonequilibrium thermodynamics [3], thermophoresis [4–6], and the propulsion of active matter [7]. Thermo-osmosis is usually described phenomenologically as the induced slippage of fluid along an interface, due to an applied temperature gradient. Phoretic motion is driven by the interfacial stresses induced by a temperature gradient in a microscopic boundary region, where the properties of the solvent are influenced by the interactions with the surface (or interface) [4–6].

Clearly, it would be useful to be able to predict thermo-osmotic slip on the basis of a molecular description of the solid-liquid interface. However, in practice this is not simple, because much of the existing theoretical framework is couched in terms that assume the validity of a local continuum theory [e.g., Debye-Hückel plus the (Navier-) Stokes equation] and make drastic assumptions about the excess enthalpy density and viscosity near the surface [8]. Yet, crucially, near an interface, a continuum description of the structure or dynamics of a liquid is not allowed. More ominously, the definition of the stress in a liquid is not unique. This nonuniqueness has no effect on the computed value of, say, the liquid-liquid surface tension [9], but it could affect the prediction of phoretic flows, where the *local* value of the stress gradient is what drives the flow. In this Letter, we consider this problem and explore novel "microscopic" methods to predict thermo-osmotic slippage in a simple model system.

The "classical" approach to predict thermo-osmotic slippage is based on Onsager's reciprocity relations (see Ref. [10]). These relations have previously been used in molecular simulations to compute diffusio-osmotic slip [2]. Derjaguin [11] used Onsager's linear nonequilibrium thermodynamics (LNET) approach to derive an expression for thermo-osmotic slip. His approach exploits the relation between the flow caused by a temperature gradient and the excess heat flux due to hydrodynamic flow, resulting in the following equation:

$$v_s = -\frac{2}{\eta} \int_0^\infty dz z \Delta h(z) \frac{\nabla T}{T}, \tag{1}$$

where $\Delta h(z)$ is the excess enthalpy density at a height z above the surface and η is the viscosity. The difficulty with this expression is that there is some ambiguity in the microscopic definition of the local excess enthalpy $\Delta h(z)$, a quantity that is also not easy to probe in experiments [4].

The key motivation for our work is that, while a continuum approximation to Eq. (1) may be sufficient for interaction lengths on the order of tens of nanometers, it does not work for atomic or molecular liquids that do not contain free charges. Rather, the excess enthalpy density $\Delta h(z)$ is a function of the solvent polarity [12], liquid structure in the boundary layer [8], temperature, and pressure. Additionally, the viscosity η can vary dramatically near a (structured) surface. Our approach circumvents all these issues: We argue that the numerical tools that we use can be applied to realistic models that cannot be described using continuum approaches.

To place the various descriptions of thermo-osmotic slip in a broader context, we first consider the classical thermodynamic approach to the problem, based on the assumption of local thermal equilibrium (LTE). We note that neither temperature gradients nor, for that matter, chemical potential gradients can exert a net force on a fluid element in a bulk liquid. Mechanical forces in liquids can be caused only by body forces such as gravity or by pressure gradients. If temperature gradients cause flow near a surface, it is only because a local pressure gradient is induced. To clarify this, we first consider the thermodynamics of the problem. Consider a temperature gradient $+x$ direction parallel to a hard wall; the z coordinate measures distance perpendicular to the wall. Dividing the Gibbs-Duhem relation for an n-component mixture by V and differentiating with respect to x gives

$$\frac{\partial P}{\partial x} = \left(\sum_{i=1}^n \rho_i \frac{\partial \mu_i}{\partial T} + \frac{S}{V} \right) \frac{\partial T}{\partial x}, \tag{2}$$

where ρ_i is the number density of species i. The Gibbs-Duhem equation makes use of the fact that the system is homogeneous. A stratified system in equilibrium is homogeneous in the directions parallel to the stratification but not perpendicular to it. Hence, here and in what follows, the "pressure" P refers to a component of the pressure tensor parallel to the surface (e.g., P_{xx}). In the bulk, the pressure is equalized quickly, and the fluid reaches hydrostatic equilibrium. Since the bulk pressure is constant, Eq. (2) reduces to

$$\left(\frac{\partial \mu_i}{\partial T}\right)_P = -s_i^B \quad (3)$$

using $S = \sum_i N_i s_i$, where s_i is the specific entropy of species i and the superscript B denotes a bulk quantity. At a position z above the surface, the pressure gradient remains. Assuming that there are no gradients of μ_i and T perpendicular to the surface, Eq. (3) can be substituted into Eq. (2) to give

$$\frac{\partial P(z)}{\partial x} = \left(-\sum_{i=1}^{n} \rho_i(z) s_i^B + \sum_{i=1}^{n} \rho_i(z) s_i(z)\right)\frac{\partial T}{\partial x}. \quad (4)$$

Equation (4) can be simplified by noting that the expression in brackets is the difference between the specific entropy at position z and the bulk specific entropy. Since μ_i and T do not depend on z, $\mu_i = h_i - Ts_i$ can be used to rewrite Eq. (4) as

$$\frac{\partial P(z)}{\partial x} = \left(\frac{\sum_{i=1}^{n}\rho_i(z)[h_i(z) - h_i^B]}{T}\right)\frac{\partial T}{\partial x} \quad (5)$$

$$= \left(\frac{\Delta h(z)}{T}\right)\frac{\partial T}{\partial x}, \quad (6)$$

where $\Delta h(z)$ is the excess enthalpy density at a distance z from the surface. To compute the flow velocity, we integrate the expression for the pressure gradient using the linearized (Navier-)Stokes equation giving

$$v_s = -\frac{1}{\eta}\int_0^\infty dz \, z \left(\frac{\Delta h(z)}{T}\right)\frac{\partial T}{\partial x}. \quad (7)$$

This is equivalent to Eq. (1) apart from a factor of 2. The factor of 2 in Derjaguin's result arises from his missing a factor of $1/2$ in his expression for Poiseuille flow [11].

To relate our LTE expression to Derjaguin's LNET approach, consider the slit pore as depicted in Fig. 1. A pressure and temperature gradient is maintained across the slit. Fluid flows in the $-x$ direction as depicted by the arrows. For a one-component fluid, the resulting phenomenological equations are
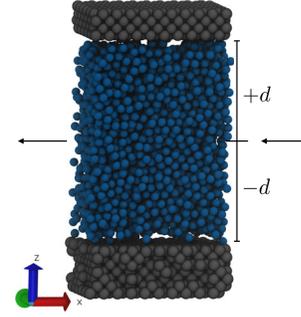
FIG. 1. Atomic fluid (blue) interacting with solid walls (gray) in a slit pore. $2d$ is the gap width.

$$v_x = -\beta_{11}\nabla P - \beta_{12}\frac{\nabla T}{T}, \quad (8)$$

$$Q_x = -\beta_{21}\nabla P - \beta_{22}\frac{\nabla T}{T}, \quad (9)$$

where v_x is the fluid velocity (m/s) and Q_x is the heat flux [J/(m^2 s)]. Following Derjaguin [11], by considering the isothermal heat flux across the pore, β_{21} can be expressed as

$$\beta_{21} = -\left(\frac{Q_x - h^B v_x}{\nabla P}\right)_T. \quad (10)$$

β_{21} defined here is conventionally known as the "mechano-caloric" coefficient. Similarly, by considering the isobaric mass flux in Eq. (8), we can write

$$\beta_{12} = -\left(\frac{v_x}{(\nabla T/T)}\right)_P. \quad (11)$$

Assuming that the hydrodynamic flow in Eq. (10) is linear in the boundary layer $v_x(z) = -dz\nabla P/\eta$ and substituting Eq. (7) for v_x in Eq. (11) immediately shows $\beta_{12} = \beta_{21}$ as expected. This provides the link between our LTE and Derjaguin's LNET approach.

The usual definition of the "slip" velocity is the extrapolated velocity at the interface, where the fluid density approaches zero. For a thin boundary layer, the slip velocity is equal to the fluid velocity in the bulk just outside the boundary layer. β_{12} in Eq. (11) is the "thermo-osmosis" coefficient.

Of course, the analytical theory given by Eqs. (5)–(7) is inappropriate for a molecular description of slip. The viscosity η is not constant near the interface. To avoid making such continuum assumptions, we compute the thermo-osmotic slip, using a mechanical route, i.e., by computing the force on a volume element directly from the gradient of the microscopic stress. Such an approach could be problematic due to the nonuniqueness of the definition of the microscopic stress. Han [13] postulated a similar approach; however, he did not validate his results.

We start with the relation between the stress gradient and $f_x(z)$, the force per unit volume on a fluid element at a distance z from the surface. Rather than computing the stress gradient in a nonequilibrium simulation, we use the fact that P_{xx} depends on x, only through T. Hence,

$$f_x(z) = -\left(\frac{P_{xx}^{eq,T_2}(x,z) - P_{xx}^{eq,T_1}(x,z)}{T_2 - T_1}\right)\left(\frac{\partial T}{\partial x}\right), \quad (12)$$

where the superscript eq denotes equilibrium calculations that are both carried out at the same bulk pressure. With this method, $\Delta P/\Delta T$ is determined, and for any $\partial T/\partial x$, $f_x(z)$ can be computed via Eq. (12). The thermo-osmotic force per particle $f_x^P(z) = f_x(z)/\rho_{ave}(z)$, where $\rho_{ave}(z) = [\rho(T_1, z) + \rho(T_2, z)]/2$. To compute the thermo-osmotic flow, we carry out a second simulation at the average temperature $T_{ave} = (T_1 + T_2)/2$, where we apply the local body force $f_x^P(z)$ to fluid particles. The resulting slip velocity and therefore β_{12} can then be computed.

The calculation as described above is complicated by the fact that the pressure tensor in an inhomogeneous fluid is not unique [14,15]. Irving and Kirkwood (IK) [16] proposed an expression by integrating the total momentum flux acting across a virtual surface element. This approach gives the appropriate mechanical force balance normal to the interface. However, as argued by Schofield and Henderson [9], the definition of the pressure tensor is not unique, since any term with a vanishing divergence can be added without changing the momentum flux. All common definitions do, however, yield the correct surface tension.

In a simulation, we need to know the thermo-osmotic force acting on atoms, as opposed to the force on the fictitious surface of a volume element. This would suggest that the atom-based virial (V) expression for pressure might be preferable.

In order to determine if the choice of the pressure affects the computed thermo-osmosis coefficient, we computed P_{xx} in Eq. (12) using both the V and IK expressions. The V pressure is given by [17]

$$P_{xx}^V(z) = \langle\rho(z)\rangle k_B T - \frac{1}{2V(z)}\left\langle\sum_i^{N(z)}\sum_{j\neq i}\frac{x_{ij}^2}{r_{ij}}\phi'(r_{ij})\right\rangle, \quad (13)$$

where r_{ij} is the distance between atoms i and j, x_{ij} is the distance in x, $\phi(r_{ij})$ is the interaction potential between the atoms, and $V(z)$ and $N(z)$ are the bin volume and number of atoms, respectively, in the bin at position z. The IK pressure is computed using [18]

$$P_{xx}^{IK}(z) = \langle\rho(z)\rangle k_B T$$
$$- \frac{1}{2A}\left\langle\sum_i^N\sum_{j\neq i}\frac{x_{ij}^2}{r_{ij}}\frac{\phi'(r_{ij})}{|z_{ij}|}\Theta\left(\frac{z-z_i}{z_{ij}}\right)\Theta\left(\frac{z_j-z}{z_{ij}}\right)\right\rangle. \quad (14)$$

In addition to these "mechanical" expressions for the thermo-osmotic force, consider the right-hand side of Eq. (5). We express the local specific enthalpy as

$$h(z) = u(z) + \frac{P_{xx}^V(z)}{\rho(z)}, \quad (15)$$

where u is the specific internal energy. In Eq. (15), we have made explicit that the pressure that enters into the expression for the local enthalpy must be the component that is parallel to the surface, as argued below Eq. (2). The body force on a fluid element at a height z above the surface is then given by

$$f_x(z) = -\frac{\rho(z)[h(z) - h^B]}{T}\left(\frac{\partial T}{\partial x}\right). \quad (16)$$

Equation (16) can be computed in a simulation thermostated at T_{ave} and applied as a body force in the same vein as Eq. (12).

We compare the above calculations of the slip coefficient with the result for β_{21} that follows from Derjaguin's approach based on the Onsager reciprocity relations. In this case, a uniform pressure gradient represented by a body force is applied during a simulation at T_{ave}. β_{21} is computed via Eq. (10) (see Supplemental Material S2 [19]). The mechanical and LTE approaches for computing β_{12} and the "Derjaguin" method for computing β_{21} should be equivalent if the temperature and pressure gradients are small enough to ensure that the resulting response is linear. Thus, we also include in this Letter the first molecular simulation of the mechanocaloric effect.

All molecular dynamics simulations reported here were performed using the LAMMPS package [20]. The simulation setup is depicted in Fig. 1. The system consists of $N = 2640$ fluid atoms interacting with other fluid atoms and solid atoms via a truncated and shifted Lennard-Jones potential:

$$V_{trunc}(r) = \begin{cases} 4\epsilon[(\frac{\sigma}{r})^{12} - (\frac{\sigma}{r})^6] - V(r_c) & r \leq r_c, \\ 0 & r > r_c, \end{cases} \quad (17)$$

where $r_c = 4\sigma$, $\sigma_{fluid-fluid} = \sigma_{solid-fluid} = \sigma$, and $\epsilon_{fluid-fluid} = \epsilon$. Two different wall-fluid interactions were investigated: a less attractive Lennard-Jones potential where $\epsilon_{solid-fluid} = 0.55\epsilon$ and a purely repulsive Weeks-Chandler-Andersen (WCA) potential [21] such that $r_c = 2^{1/6}\sigma$ for solid-fluid interactions. Solid atoms are bonded via harmonic springs to their nearest neighbors in an fcc lattice of density $0.9\sigma^{-3}$. The stiffness $k_{bond} = 5000\epsilon/\sigma^2$, and the rest length is 1.1626σ. All computed quantities are expressed in Lennard-Jones reduced units.

NVT dynamics with a time step $\Delta t = 0.001\tau$ were run to equilibrate the system. This was accomplished using a Nosé-Hoover thermostat for 100 000 MD steps. For an additional 100 000 steps, the system was barostated at
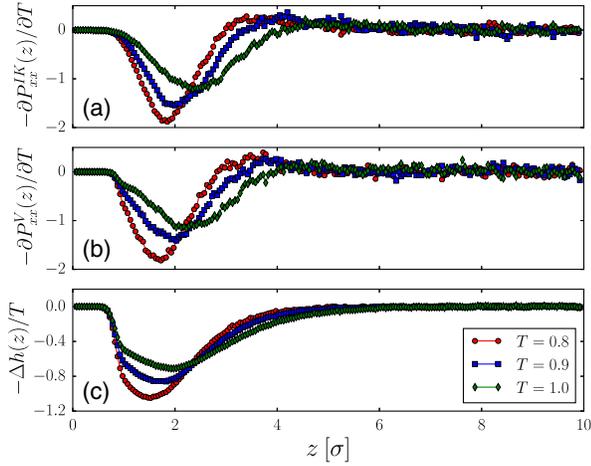
FIG. 2. $-\Delta P_{xx}(z)/\Delta T$ $[k_B/\sigma^3]$ computed using the (a) IK and (b) V pressure tensor; e.g., the profile for $T = 0.8$ is computed by taking the difference in P_{xx} at $T = 0.85$ and 0.75 and dividing by $\Delta T = 0.1$. (c) WCA wall-fluid interactions significantly exclude volume and thereby create a large enthalpy difference at the surface. The solid wall is located at $z \sim 0$.

$P \approx 0.122$ by applying a downward force to the top wall atoms.

Using the pressure profiles [see Supplemental Material, Figs. S1(a) and S1b) [19]], $\Delta P_{xx}(z)/\Delta T$ was computed for the three temperatures shown in Figs. 2(a) and 2(b). Encouragingly, the choice of the pressure tensor makes no significant difference to the measured response.

At constant temperature T_{ave}, the specific kinetic energy is uniform everywhere and therefore computed by dividing the total average kinetic energy by the number of atoms. For the same temperatures, the specific potential energy profiles were spatially averaged in z. Using the profiles of P_{xx} [Fig. S1(a) [19]] and density profiles [Fig. S1(c) [19]], $\Delta h(z)/T$ was computed via Eqs. (15) and (16) and shown in Fig. 2(c).

We note that the V and IK expressions [Figs. 2(a) and 2(b)] and the LTE quantity [Fig. 2(c)] show similar qualitative behavior. The body force vanishes in the bulk, and the profiles flatten and shift outward as the temperature is increased.

The body force per particle $f_x^P(z)$ can be computed by dividing the profiles in Figs. 2(a)–2(c) by $\rho(z)$ [Fig. S1(c) [19]] and multiplying by a sufficiently small gradient, e.g., $\partial T/\partial x = 0.0005$ for WCA wall-fluid interactions. To compute slip, nonequilibrium simulations were carried out by applying these forces to the equilibrated systems at the appropriate temperatures. To obtain reasonable statistics, forces were applied for 10^8 steps until the fluid approached a steady velocity. The slip was then computed for an additional 2×10^8 steps.

Figures 3(a) and 3(c) show calculations of the slip velocity. Interestingly, although the mechanical and LTE approaches give different force profiles (Fig. 2), they predict
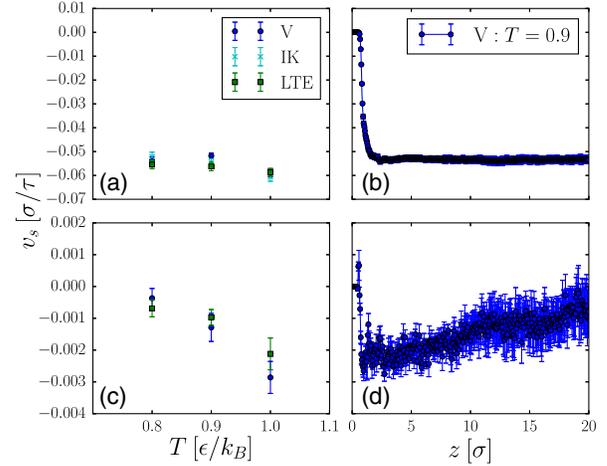
FIG. 3. Calculations of the slip velocity and flow profile for different wall-fluid interactions: (a),(b) WCA at $\nabla T = 0.0005$ and (c),(d) Lennard-Jones ($\epsilon_{wf} = 0.55\epsilon$) at $\nabla T = 0.003$.

the same velocity far away from the surface. The flow profile computed at $T = 0.9$ [Fig. 3(b)] shows that for WCA wall interactions the velocity decreases monotonically, indicating that the viscosity close to the surface is constant. For less attractive Lennard-Jones [Fig. 3(d)], the viscosity and forces are clearly not constant showing significant departure from (Navier-)Stokes and Derjaguin's result [Eq. (1)].

To compare our stress gradient and LTE approaches with Derjaguin's method (see Supplemental Material S2 [19]), β_{12} was computed via Eq. (11) using the slip calculations shown in Figs. 3(a) and 3(c). Figure 4 shows a comparison of all three methods. For the range of temperatures, there appears to be reasonable agreement. For $T \sim 96-120$ K in argon units, the thermo-osmosis coefficient ranges from
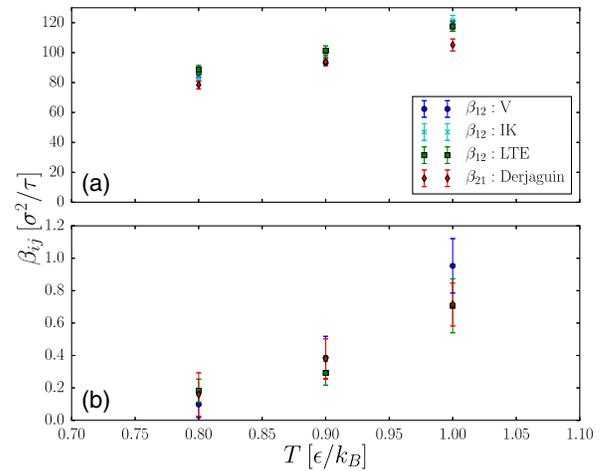
FIG. 4. Comparison of Onsager reciprocal relations, β_{12} computed via our stress gradient (circles, crosses) and LTE (squares) approaches and β_{21} calculated by following Derjaguin's LNET method (diamonds). Thermo-osmosis coefficients are computed for (a) WCA ($\nabla T = 0.0005$, $\nabla P = 0.00004$) and (b) Lennard-Jones ($\nabla T = 0.003$, $\nabla P = 0.0005$) interactions.

0.85–3.8×10^{-8} m^2/s for less attractive Lennard-Jones and 4.2–5.6×10^{-6} m^2/s for WCA walls.

As expected, the slip velocities for solely repulsive wall-fluid interactions are considerably larger than those for interactions with an attractive component. Furthermore, both cases demonstrate an approximately linear dependence of the thermo-osmosis coefficient with respect to the temperature.

In addition to the methods described above, we also attempted to compute β_{21} using the linear-response theory [22]. However, no reliable results were obtained, as the statistical noise overwhelmed the signal.

Previous molecular-simulation studies of thermal transport have dealt with the Soret coefficient of atomic species [23,24]. One cannot directly compare the Soret coefficient S_T with our computed values of the thermo-osmosis coefficient β_{12}, since the separation between excess and bulk enthalpy density becomes meaningless if all particles have the same size. As a rough comparison, given that $S_T = (\beta_{12}/T)/D_{Ar}$, taking the average of our computed values of β_{12} for $T = 0.8$ and 0.9 and using $D_{Ar} \simeq 2.47 \times 10^{-5}$ cm^2 s^{-1} as reported in Ref. [24], we compute $S_T \sim 0.047$ K^{-1}, which is the same order of magnitude as $S_T \sim 0.014$ K^{-1} at $T = 0.85$ reported by Ref. [24].

In summary, we have considered three different methods to compute thermo-osmotic slip on the basis of molecular simulations. The first approach is based on a computation of the thermally induced stress gradient method, computed using equilibrium simulations and then represented as a body force in nonequilibrium simulations. We find no evidence that different choices for the pressure tensor lead to different results. In the second approach, we compute the excess enthalpy density near the wall and use a local-thermodynamics formalism to derive the body force acting on the fluid. These methods do not assume that macroscopic thermodynamics or hydrodynamics holds close to an interface. The final approach is based on Onsager's reciprocal relations, which allow us to derive thermo-osmotic slip from the excess heat flux due to a pressure gradient.

The key results are encouraging and surprising: For certain wall-fluid interactions, the thermo-osmotic flow profile does not monotonically depend on the distance from the surface, indicating that the viscosity and forces near the surface are not constant. Furthermore, we find that all methods yield results for the thermo-osmosis coefficient that do not differ significantly. Hence, the choice of the method to compute thermo-osmotic slip seems to be a matter of taste or convenience.

The data presented in this work was generated using LAMMPS, which is publicly available at [25].

---

*Corresponding author.
rg468@cam.ac.uk
†df246@cam.ac.uk

[1] J. Morthomas and A. Würger, J. Phys. Condens. Matter **21**, 035103 (2009).
[2] A. Ajdari and L. Bocquet, Phys. Rev. Lett. **96**, 186102 (2006).
[3] J. Dhont, S. Wiegand, S. Duhr, and D. Braun, Langmuir **23**, 1674 (2007).
[4] J. Anderson, Annu. Rev. Fluid Mech. **21**, 61 (1989).
[5] R. Piazza and A. Parola, J. Phys. Condens. Matter **20**, 153102 (2008).
[6] A. Würger, Rep. Prog. Phys. **73**, 126601 (2010).
[7] R. Golestanian, T. Liverpool, and A. Ajdari, New J. Phys. **9**, 126 (2007).
[8] A. P. Bregulla, A. Würger, K. Günther, M. Mertig, and F. Cichos, Phys. Rev. Lett. **116**, 188303 (2016).
[9] P. Schofield and J. Henderson, Proc. R. Soc. A **379**, 231 (1982).
[10] S. de Groot and P. Mazur, *Non-equilibrium Thermodynamics* (North-Holland, Amsterdam, 1962).
[11] B. Derjaguin, N. Churaev, and V. Muller, *Surface Forces* (Plenum, New York, 1987).
[12] S. A. Putnam and D. G. Cahill, Langmuir **21**, 5317 (2005).
[13] M. Han, J. Colloid Interface Sci. **284**, 339 (2005).
[14] B. Hafskjold and T. Ikeshoji, Phys. Rev. E **66**, 011203 (2002).
[15] J. Rowlinson and B. Widom, *Molecular Theory of Capillarity* (Dover, New York, 2003).
[16] J. Irving and J. Kirkwood, J. Chem. Phys. **18**, 817 (1950).
[17] J. Hansen and I. McDonald, *Theory of Simple Liquids* (Elsevier, New York, 1990).
[18] J. Walton, D. Tildesley, J. Rowlinson, and J. Henderson, Mol. Phys. **48**, 1357 (1983).
[19] See Supplemental Material at http://link.aps.org/supplemental/10.1103/PhysRevLett.119.038002 for details on the calculation of the V and IK pressure profiles and a description of the "Derjaguin" method.
[20] S. Plimpton, J. Comput. Phys. **117**, 1 (1995).
[21] J. Weeks, D. Chandler, and H. Andersen, J. Chem. Phys. **54**, 5237 (1971).
[22] J. Luttinger, Phys. Rev. **135**, A1505 (1964).
[23] F. Römer, Z. Wang, S. Wiegand, and F. Bresme, J. Phys. Chem. B **117**, 8209 (2013).
[24] D. Reith and F. Müller-Plathe, J. Chem. Phys. **112**, 2436 (2000).
[25] http://lammps.sandia.gov.